Received: 17 July 2018 | Revised: 11 December 2018 | Accepted: 23 January 2019

DOI: 10.1002/ett.3586

RESEARCH ARTICLE

WILEY

USTLD mapper design for APSK constellations over satellite links

Tahmid Quazi | Sulaiman Saleem Patel

School of Engineering, University of KwaZulu-Natal, Durban, South Africa

Correspondence
Tahmid Quazi, School of Engineering, University of KwaZulu-Natal, Durban 4041, South Africa.
Email: quazit@ukzn.ac.za

Abstract

Space-time block code (STBC)–based multiple-input–multiple-output techniques have been considered recently to enhance the performance of mobile satellite communication systems in terms of link reliability. Uncoded space-time labelling diversity (USTLD) is a diversity technique that is a direct extension of the STBC system and further improves its performance. A USTLD system is proposed in this paper that is designed specifically for satellite to mobile station links. The circular M-ary Amplitude Phase-Shift Keying (MAPSK) constellation, which is adopted by the most recent satellite broadcasting standard Digital Video Broadcasting standard for nonlinear satellite links (DVB-S2X), is applied to the USTLD system. The most critical aspect of developing a USTLD system is the design of the secondary mapper to achieve labelling diversity. Existing square M-ary Quadrature Amplitude Modulation (MQAM) approaches to USTLD mapper design are adapted for appropriate 16APSK and 64APSK constellations from the DVB-S2X standard. Various metrics are derived to quantitatively compare mapper designs for a Nakagami-q fading channel. Theoretical results, verified by Monte Carlo simulations, show that the best of the MAPSK USTLD mappers considered achieve a gain of approximately 4 dB for 16APSK and 5 dB for 64APSK when compared to the Alamouti STBC system. Furthermore, a study is conducted to analytically compare USTLD mappers using the derived metrics for both MQAM and MAPSK. It is concluded that a two-stage approach is the most accurate methodology for comparing USTLD mapper designs.

1 | INTRODUCTION

In the context of Africa, satellite technology has historically played a key role in reducing the digital divide between the continent's least developed economies and the rest of the developed world.[1-3] Due to its ability to cost effectively provide wide coverage, satellite communications will be pivotal in facilitating services such as e-learning,[4] e-commerce, telehealth,[5,6] and general video broadcasting across the rural and remote areas of Africa.[7,8] Satellite technology will also be integrated into future 4G and 5G terrestrial networks, extending their range and enhancing their services.[9-12] With this goal in mind, there has been notable research interest in applying advances in multiple-input–multiple-output (MIMO) technology developed for terrestrial links for their satellite variants.[13,14] This is a nontrivial task due to limited space being available on the satellites. However, the two transmit antenna space-time block code (STBC)–based MIMO architecture

proposed by Alamouti[15] has been considered for mobile satellite communications, using polarisation diversity[13] and a two transmit antenna structure.[14] Uncoded space-time labelling diversity (USTLD) is a recently proposed MIMO technique that is a direct extension of the Alamouti STBC. It is shown by Xu et al[16] that, using a constellation with two different binary mappings, USTLD achieves significant error performance gains over the Alamouti STBC system, which only uses a single mapper. The aim of this paper is to propose a USTLD scheme specifically designed for the mobile satellite communications architecture considered by Arti and Jindal.[14]

The most common modulation scheme applied in many of the proposed labelling diversity systems, whether coded[17-21] or uncoded,[16,22-28] has been M-ary Quadrature Amplitude Modulation (MQAM). However, it is well accepted that circular constellations are more suited for satellite links than square or rectangular ones. Due to their reduced number of amplitude levels, circular constellations have a lower peak-to-average power ratio (PAPR) when compared to square or rectangular QAM modulation schemes with the same modulation order.[29] A low PAPR is desirable as high-gain power amplifiers at the satellite exhibit nonlinear characteristics when operating near their saturation region.[30] Thus, the latest Digital Video Broadcasting standard for nonlinear satellite links (DVB-S2X) uses the circular Amplitude Phase-Shift Keying (APSK) modulation scheme.[31,32]

The first contribution of this paper is to propose an APSK-based USTLD satellite system, which to the best of the authors' knowledge, has not been done prior to this. The most critical aspect of developing a USTLD system, given a modulation scheme, is the design of the two mappers used to achieve labelling diversity. The proposed mapper design exploits the similarity in structure between square MQAM and certain M-ary Amplitude Phase-Shift Keying (MAPSK) constellations from the DVB-S2X standard. In particular, these constellations consist of symbols arranged in a series of concentric squares (for MQAM) and circles (for MAPSK). This allows the heuristic-based algorithms used in the MQAM case[16,22] to be adapted for the appropriate MAPSK constellations. The second contribution of this paper is to study the performance of the proposed system using the Nakagami-q fading channel model, which has previously been done for non-MAPSK USTLD systems.[27] Chytil[33] discusses that Nakagami-q provides a good fit for modelling signal propagation in satellite transmissions subjected to strong ionospheric scintillation. The performance study, presented using theory and simulation results, compares various mapper design options and presents the best USTLD MAPSK mapper design.

A shortcoming in current USTLD literature is that there has been no attempt at developing an analytical means of comparing mapper designs. The next contribution of this paper is to address this problem by deriving a set of possible metrics for quantitatively evaluating the suitability of labelling diversity mapper designs for USTLD systems. The metrics are based on the minimum product Euclidean distance (PED) that has been used in all of the previous MQAM mapper design schemes.[16,22,23]

The rest of this paper is organised as follows. Section 2 presents the USTLD system model. Section 3 discusses the mapper design metrics and their theoretical expressions. Section 4 presents the average bit error rate (BER) performance of the proposed system for various mapper design options, modulation and channel parameters, as well as a quantitative analysis of the various USTLD mapper design metrics. Finally, Section 5 draws conclusions from the study and proposes future work.

2 | SYSTEM MODEL

The novelty of labelling diversity systems is that they achieve diversity by utilising two constellations with different binary mappings to encode the information being transmitted.[16] An m-bit information codeword (or label) L is passed through two mappers Ω_1 and Ω_2 to produce the respective symbols $\Omega_1(L)$ and $\Omega_2(L)$.

In the proposed USTLD system, two code words $\left(L_{(1)} \text{ and } L_{(2)}\right)$ are transmitted over two consecutive time slots, with Ω_1 and Ω_2 being used in time slots 1 and 2, respectively. The constellation symbols are from an MAPSK modulation scheme within the DVB-S2X standard.[31] An MAPSK constellation is characterised by the positioning of the symbols on multiple concentric rings. The 16APSK constellation considered in this paper is the 4+12 configuration in which 4 symbols are uniformly spaced on the inner ring with radius R_1 and 12 on the outer ring with radius R_2. The 64APSK constellation uses the 4+12+20+28 configuration with 4, 12, 20, and 28 symbols uniformly spaced on 4 rings with radii R_1 (innermost ring) to R_4 (outermost ring). The radii $R_1 = 1.0$ and $R_2 = 3.0$ are used for 16APSK. Similarly, $R_1 = 1.0, R_2 = 2.4, R_3 = 4.3$, and $R_4 = 7.0$ for 64APSK. These values fall within the range recommended by the standard.[31] Before transmission, the symbols are normalised to ensure that $E\left\{|\Omega_1(L)|^2\right\} = E\left\{|\Omega_2(L)|^2\right\} = 1$ for all possible labels $L \in [0 : 2^m - 1]$, where $|\cdot|$ and $E\{\cdot\}$ represent the Euclidean norm and the expectation, respectively.

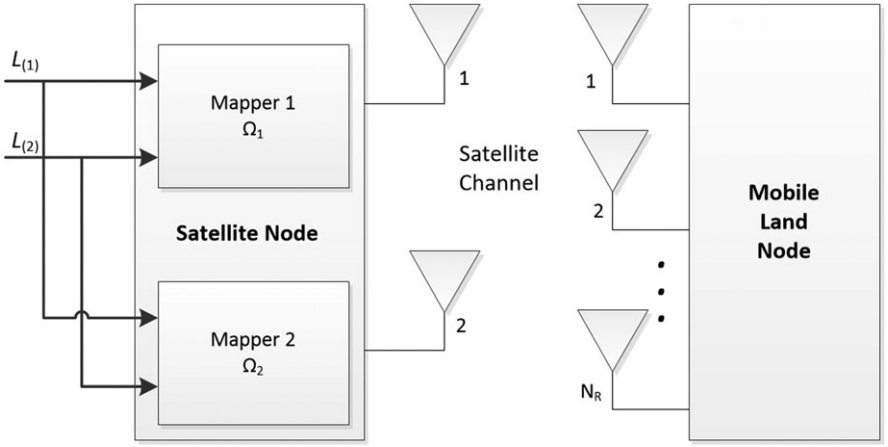

FIGURE 1 System model

The system model in Figure 1 considers a MIMO architecture with two transmit antennas at the satellite station and N_R receive antennas at the mobile land station. Thus, the $N_R \times 1$ received signal vector, $\mathbf{y}$, in time slot t is given by

$$\mathbf{y}_t = \sqrt{\frac{\rho}{2}} \left[\mathbf{h}_{t,1}\ \Omega_t\left(L_{(1)}\right) + \mathbf{h}_{t,2}\ \Omega_t\left(L_{(2)}\right)\right] + \mathbf{n}_t,\ \ t \in [1:2]. \tag{1}$$

In (1), $\sqrt{\frac{\rho}{2}}$ is the average signal-to-noise ratio (SNR) at each receiver antenna and $\mathbf{n}$ is the $N_R \times 1$ additive white Gaussian noise vector. The entries of $\mathbf{n}$ are independent and identically distributed complex Gaussian random variables with zero mean and a variance of 0.5 per dimension.

The $N_R \times 1$ vector $\mathbf{h}_{t,i}$, t, $i \in [1:2]$, represents the multipath fading experienced by the symbol transmitted from antenna i during time slot t. The fading is assumed to follow a uniform phase distribution and a Nakagami-q amplitude distribution, the probability density function for which is given by

$$f_x(x) = \frac{x\left(1+q^2\right)}{q} \exp\left(-\frac{x^2\left(1+q^2\right)^2}{4q^2}\right) I_0\left(\frac{x^2(1-q^4)}{4q^2}\right), \tag{2}$$

where x is the fading amplitude, $I_0(\cdot)$ is the modified zeroth-order Bessel function of the first kind,[34] and the fading parameter, q, is the energy ratio of the quadrature component of the fading to its in-phase component[27] and should be in the range $0 \leq q \leq 1$. The Nakagami-q fading model provides a good fit for modelling signal propagation in satellite transmissions subjected to strong ionospheric scintillation.[33] Furthermore, Nakagami-q allows more insight into the worst-case error performance of the system and is thus used ahead of the more common Rayleigh fading model.[27] The fading channels are assumed to be frequency flat and may be either fast fading or quasi-static over the duration of the two time slots.

At the receiver, maximum-likelihood detection is used to estimate the transmitted information codewords. Assuming that perfect channel state information is available at the receiver, detection may be described according to

$$\widetilde{L}_{(1)}, \widetilde{L}_{(2)} = \underset{\hat{L}_{(1)}, \hat{L}_{(2)} \in [0:2^m-1]}{\operatorname{argmin}} \left\| \mathbf{y}_1 - \sqrt{\frac{\rho}{2}} \sum_{u=1}^{2} \mathbf{h}_{u,1}\ \Omega_1\left(\hat{L}_{(u)}\right) \right\|^2 + \left\| \mathbf{y}_2 - \sqrt{\frac{\rho}{2}} \sum_{u=1}^{2} \mathbf{h}_{u,2}\ \Omega_2\left(\hat{L}_{(u)}\right) \right\|^2, \tag{3}$$

where $\|\cdot\|$ denotes the vector Frobenius norm. The estimated codewords are denoted as $\widetilde{L}_{(1)}$ and $\widetilde{L}_{(2)}$, and similarly, the candidate labels to be tested during the detection are denoted $\hat{L}_{(1)}$ and $\hat{L}_{(2)}$. The maximum-likelihood detection incurs a complexity of $M^2(40\,N_R - 1)$ effective real operations, which is derived using eq. (29) in the work by Patel et al.[26] By comparison, the system described by Arti and Jindal[14] also incurs the same complexity under fast fading conditions. However, under quasi-static conditions, the orthogonal structure of the system by Arti and Jindal allows signals to be decoupled, which allows for lower complexity detection.

3 | MAPPER DESIGN

The design of the two binary mappers Ω_1 and Ω_2 determines the extent of the diversity achieved by the USTLD system. For a given M-ary constellation with primary mapping Ω_1, there are $M!$ possible secondary mappings Ω_2, where $(\cdot)!$ represents the factorial. Xu et al[16] show that, to achieve labelling diversity, labels from Ω_1 corresponding to adjacent symbols on the constellation are spaced further apart when mapped by Ω_2. To solve this optimisation problem, Samra et al[23] applied a search algorithm that was constrained to small constellations ($M \leq 16$) due to its complexity. In comparison, Seddik et al[22] and Xu et al[16] used heuristic approaches to design mappers for higher-order constellations. The latest of these works[16] presents a comparison of the BER results achieved using these mappers but does not provide a quantitative means to evaluate the mappers. In the following discussion, various analytical metrics are derived to evaluate the quality of USTLD mappers. These will be used in Section 4 to evaluate the mappers considered in this paper.

3.1 | Metrics for mapper evaluation

The average BER of USTLD systems in Nakagami-q has been previously derived analytically. The full derivation, and its associated assumptions, is shown in appendix A in the work of Patel et al.[27] The derivation follows the union bound approach, which is given by

$$P_b(\rho) \leq \frac{1}{m2^m} \sum_{L=0}^{2^m-1} \sum_{\substack{\widetilde{L}=0 \\ \widetilde{L}\neq L}}^{2^m-1} \delta(L,\widetilde{L}) P\left(L \to \widetilde{L}\right), \tag{4}$$

where $\delta(L,\widetilde{L})$ and $P(L \to \widetilde{L})$ are respectively the number of bit errors and the pairwise error probability (PEP) between the transmitted label L and estimated label $\widetilde{L}$. It was shown by Patel et al[27] that the PEP is an integral defined in terms of the moment-generating function (MGF) of the fading distribution. The trapezoidal approximation of the PEP is given by[27]

$$P\left(L \to \widetilde{L}\right) \approx \frac{1}{4n} \prod_{i=1}^{2} \left[\mathcal{M}_i\left(\frac{1}{2}\left|d_i(L,\widetilde{L})\right|^2\right)\right]^{N_R} + \frac{1}{2n} \sum_{j=1}^{n-1} \prod_{i=1}^{2} \left[\mathcal{M}_i\left(\frac{\left|d_i(L,\widetilde{L})\right|^2}{2\sin^2\left(\frac{j\pi}{2n}\right)}\right)\right]^{N_R}, \tag{5}$$

where n is an arbitrary large integer $n > 10$ and the distance $d_i(L,\widetilde{L})$ is given by

$$d_i(L,\widetilde{L}) = \Omega_i(L) - \Omega_i(\widetilde{L}), \quad i \in [1:2], \tag{6}$$

and the MGF for a Nakagami-q distribution is given by[34]

$$\mathcal{M}_i(s) = \left[1 + \frac{s\rho}{2} + \left(\frac{sq\rho}{2(1+q^2)}\right)^2\right]^{-\frac{1}{2}}. \tag{7}$$

Similar to the approach followed by Xu et al,[16] at high SNR, the squared term in the MGF dominates. Thus, the PEP at high SNR can be approximated as

$$P\left(L \to \widetilde{L}\right) \approx \frac{1}{4n} \prod_{i=1}^{2} \left(\frac{q\rho\left|d_i\left(L,\widetilde{L}\right)\right|^2}{4\left(1+q^2\right)}\right)^{-N_R} + \frac{1}{2n} \sum_{j=1}^{n-1} \prod_{i=1}^{2} \left(\frac{q\rho\left|d_i\left(L,\widetilde{L}\right)\right|^2}{4\left(1+q^2\right)\sin^2\left(\frac{j\pi}{2n}\right)}\right)^{-N_R}. \tag{8}$$

The expression in (8) indicates that the average BER of USTLD systems at high SNRs is dominated by the PED, $\prod_{i=1}^{2}\left|d_i\left(L,\widetilde{L}\right)\right|$. Thus, the error floor of the PEP is bounded by the minimum PED. This has been used by previous works[16,22] to determine the heuristics for their mapper designs. The optimisation problem to determine the optimum secondary mapper $\left(\Omega_2^{\text{opt}}\right)$ for a USTLD system, given a primary mapper Ω_1, can then be formally stated as[16]

$$\Omega_2^{\text{opt}} = \underset{\substack{L,\widetilde{L}\in[0:2^m-1] \\ L\neq\widetilde{L}}}{\operatorname{argmax}} \ \zeta\left(L,\widetilde{L}\right), \tag{9}$$

where ζ is the mapper evaluation metric. From (4) and (8), four suitable metrics that can be applied in (9) are the following:

1. the minimum PED, given in (10);
2. the minimum bit-difference-weighted PED, given in (11);
3. the minimum summed PED, given in (12). This is directly proportional to the minimum averaged PED;
4. the minimum bit-difference-weighted summed PED, given in (13). This is directly proportional to the minimum bit-difference-weighted averaged PED.

$$\zeta^{(1)} = \min_{\substack{L,\widetilde{L}\in[0:2^m-1]\\ L\neq\widetilde{L}}} \prod_{i=1}^{2} \left| d_i\left(L,\widetilde{L}\right)\right| \tag{10}$$

$$\zeta^{(2)} = \min_{\substack{L,\widetilde{L}\in[0:2^m-1]\\ L\neq\widetilde{L}}} \prod_{i=1}^{2} \frac{1}{\delta(L,\widetilde{L})} \left| d_i\left(L,\widetilde{L}\right)\right| \tag{11}$$

$$\zeta^{(3)} = \min_{L\in[0:2^m-1]} \sum_{\widetilde{L}=0}^{2^m-1} \prod_{i=1}^{2} \left| d_i\left(L,\widetilde{L}\right)\right| \tag{12}$$

$$\zeta^{(4)} = \min_{L\in[0:2^m-1]} \sum_{\widetilde{L}=0}^{2^m-1} \prod_{i=1}^{2} \frac{1}{\delta(L,\widetilde{L})} \left| d_i\left(L,\widetilde{L}\right)\right| \tag{13}$$

Previous works[16,22] used the minimum PED to guide their mapper designs; however, in this paper, the metrics (10)-(13) are considered to evaluate the quality of possible mappers.

3.2 | Proposed mappers

There have been a number of recent studies involving the APSK modulation scheme. Sung et al[35] presented a study of symmetrical MAPSK, while Meloni et al[36,37] and Chen and Yang[38] considered the nonsymmetrical configurations of the constellation. However, as mentioned previously, there are no works that have considered MAPSK in the context of USTLD systems. It is generally difficult to design USTLD mappers geometrically as the axes of the constellations defined by each of the two mappers define a four-dimensional optimisation space.

All previous attempts at mappers designs[16,22,23] have only considered symmetrical MQAM and M-ary Phase-Shift Keying (MPSK) constellations. These designs are limited in that they either constrain the modulation order[23] or use nonoptimal heuristic-based approaches.[16,22] The formulation of a generic methodology to develop optimum USTLD mapper designs for both symmetric and nonsymmetric MAPSK is still an open research problem. In this paper, the similarity in structure between square MQAM (M = 16 and 64) constellations and their MAPSK counterparts (4+12 16APSK and 4+12+20+28 64APSK) is used to propose mapper designs for the 16-ary and 64-ary APSK USTLD systems. The proposed mapper designs rely on the observation that MQAM and MAPSK constellations consist of symbols arranged in a series of concentric squares and circles, respectively. Using this premise, the adapted repositioning of the symbols from the 16QAM constellation to the 16APSK constellation is shown in Figure 2. The same process is followed for 64APSK, as illustrated by the example for a single quadrant in Figure 3. Furthermore, Xu et al present a USTLD mapper design heuristic for circular constellations based on MPSK.[16] This has been applied for circular constellations in the most recent literature on USTLD systems.[26,27] This heuristic has also been adapted and applied for MAPSK constellations in this paper.

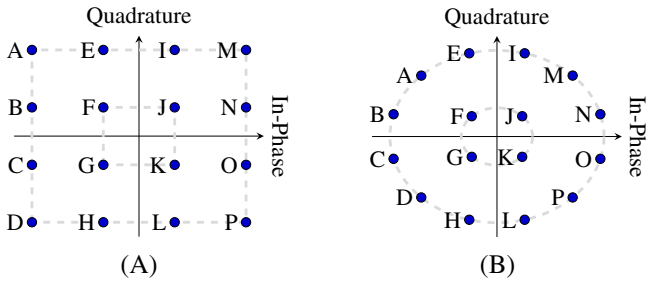

FIGURE 2 16APSK approximation of 16QAM constellation. A, 16QAM constellation; B, 16APSK constellation

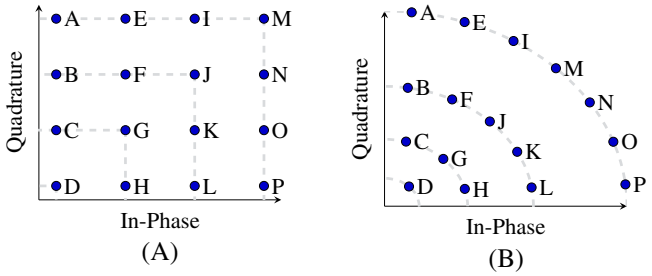

FIGURE 3 64APSK approximation of 64QAM constellation. A, One quadrant of 64QAM constellation; B, One quadrant of 64APSK constellation

Point	Ω_1	Ω_2^{Samra}	Ω_2^{Seddik}	$\Omega_2^{\text{Xu,QAM Based}}$	$\Omega_2^{\text{Xu,PSK Based}}$
A	0000	1111	0101	0000	1010
B	0001	1100	0110	1110	0001
C	0011	1110	0100	0011	0011
D	0010	1101	0111	1101	1000
E	0100	0001	1001	1011	0100
F	0101	0010	1010	0101	1111
G	0111	0000	1000	1000	1101
H	0110	0011	1011	0110	0110
I	1100	1001	0001	1100	1100
J	1101	1010	0010	0010	0111
K	1111	1000	0000	1111	0101
L	1110	1011	0011	0001	1110
M	1000	0111	1101	0111	0010
N	1001	0100	1110	1001	1001
O	1011	0110	1100	0100	1011
P	1010	0101	1111	1010	0000

(A)

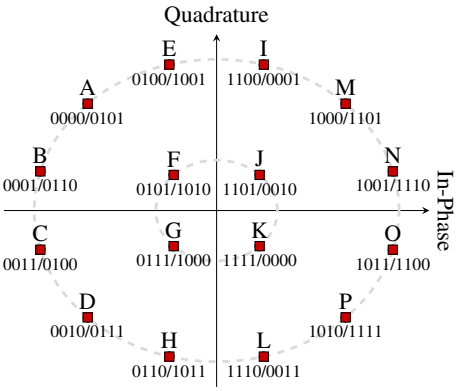

(B)

FIGURE 4 16APSK USTLD mapper design. A, Symbol-to-bit allocations for USTLD mappers; B, Example of 16APSK USTLD mappers. Key: $\Omega_1/\Omega_2^{\text{Seddik}}$. USTLD, uncoded space-time labelling diversity

Due to the similarities in their structure, the symbol-to-bit allocation for both 16-ary QAM and APSK is shown in Figure 4A. In the Figure, Ω_1 follows a conventional Gray coding bit allocation. The constellation designs for mapper 2 from Samra et al,[23] Seddik et al,[22] and Xu et al[16] are denoted by Ω_2^{Samra}, Ω_2^{Seddik}, and Ω_2^{Xu}, respectively. A visual representation of the mapper design for Ω_1 and Ω_2 based on the heuristic used by Seddik et al is illustrated in Figure 4B.

The high computation complexity of the approach used by Samra et al makes it infeasible for a 64-ary constellation.[23] Thus, only the heuristic-based approaches of Seddik et al[22] and Xu et al[16] are used to determine the symbol-to-bit allocation for 64APSK. For brevity, the symbol-to-bit allocation table for 64APSK is not shown; however, the methodology is identical

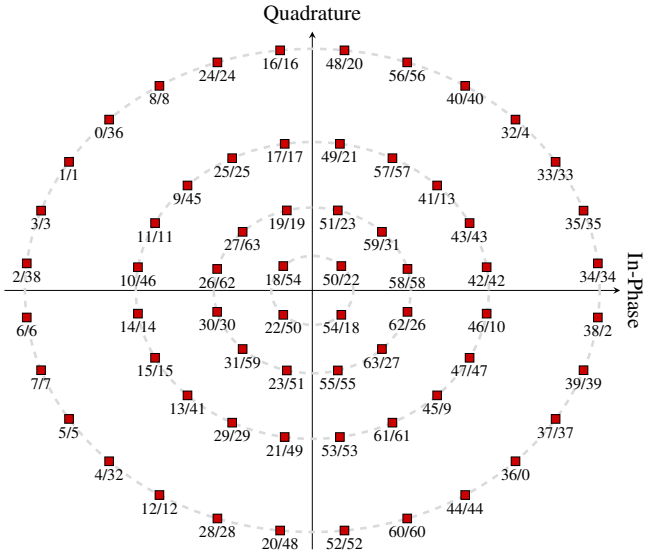

FIGURE 5 Example of 64APSK USTLD mappers. Key: $\Omega_1/\Omega_2^{\text{Xu, PSK Based}}$. USTLD, uncoded space-time labelling diversity

to that followed for 16APSK. As an example, a visual representation of the mapper design for Ω_1 and $\Omega_2^{\text{Xu, PSK Based}}$ is illustrated in Figure 5. $\Omega_2^{\text{Xu, PSK Based}}$ was chosen over the other two options $\left(\Omega_2^{\text{Xu, QAM Based}} \text{ and } \Omega_2^{\text{Seddik}}\right)$ for the example as there was significant adaptation of its heuristic for the 4+12+20+28 64APSK constellation. For ease of presentation, the decimal notation of the binary allocation for the symbols is shown for each mapper in Figure 5.

4 | RESULTS AND DISCUSSION

The performance study of the proposed system is divided into two sections. The first presents the average BER performance of the proposed MAPSK USTLD system in fast-fading Nakagami-q channels. This is benchmarked against the Alamouti STBC to show the effect of labelling diversity. This is a fair comparison as both STBC systems have the same structure, ie, a $2 \times N_R$ MIMO configuration and the use of 2 time slots to transmit information. N_R is set to 4 in the performance study. The second subsection compares the mapper designs for MQAM and MAPSK USTLD using the metrics derived in Section 3.1. The comparison is shown via quantitative evaluations of the possible metrics for each considered mapper.

The theoretical results for the BER performance presented are obtained from the union bound given in (4). Due to the use of the union bound, the analytical expression is only expected to be accurate in the high SNR region as shown in previous works.[16,26-28]

4.1 | BER performance of proposed MAPSK USTLD systems

The improvements in average BER performance achieved by the MAPSK USTLD system over the Alamouti STBC is shown in Figures 6 and 7. For 16APSK USTLD, the best performing mapper designs are Ω_2^{Samra} and Ω_2^{Seddik}. The gains achieved by these mappers at an average BER of 1×10^{-5} are approximately 4 dB for both $q = 1$ and $q = 0.1$. For 64APSK USTLD, the best performing mapper design is Ω_2^{Seddik}. The gains achieved by these mappers at a average BER of 1×10^{-5} are approximately 5 dB for both $q = 1$ and $q = 0.1$. These gains are attributed to the USTLD system using two mappers in the transmission process while the Alamouti STBC system only uses one. The results from the theoretical expression (4) for both systems are shown to closely match the results from the Monte Carlo simulations for the Nakagami-q, $q = 1$ channel at high SNRs.

In terms of the mapper design comparison, Ω_2^{Samra} and Ω_2^{Seddik} are equal for 16APSK and perform the best. The next in rank is $\Omega_2^{\text{Xu,QAM Based}}$ and the worst performing one is $\Omega_2^{\text{Xu,PSK Based}}$. For 64APSK, $\Omega_2^{\text{Xu,PSK Based}}$ is marginally better than $\Omega_2^{\text{Xu,QAM Based}}$; however, Ω_2^{Seddik} is significantly superior to both these designs.

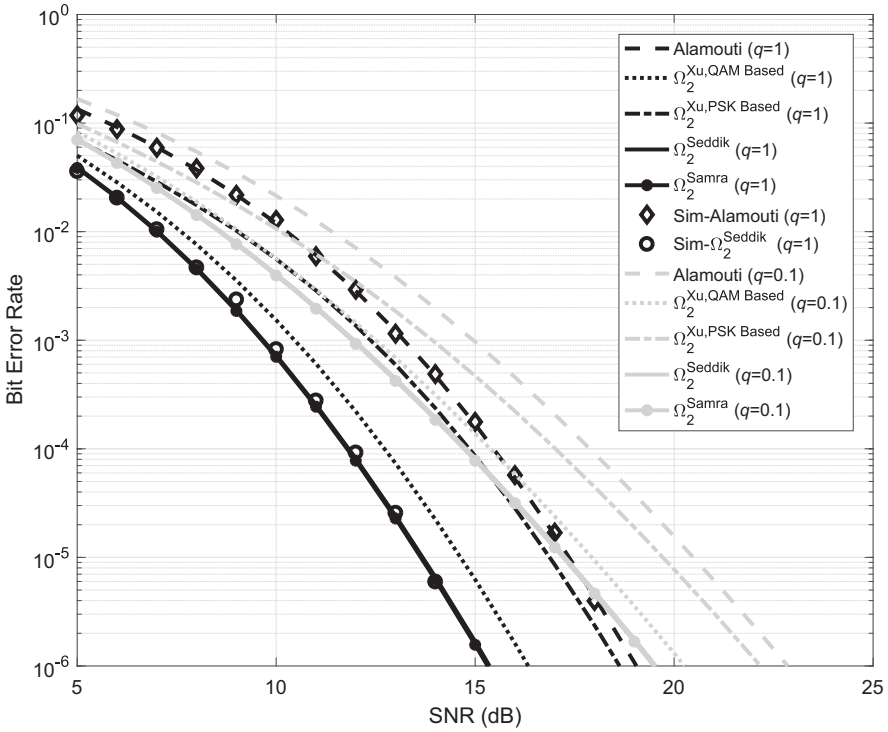

FIGURE 6 Average BER—16APSK, Nakagami-q. BER, bit error rate; SNR, signal-to-noise ratio

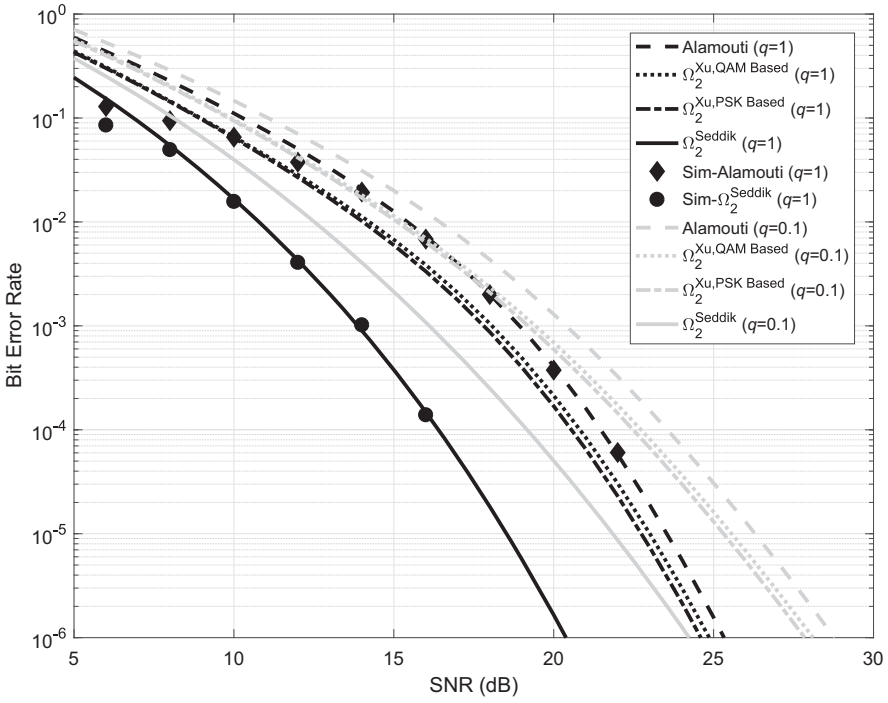

FIGURE 7 Average BER—64APSK, Nakagami-q. BER, bit error rate; SNR, signal-to-noise ratio

4.2 | Evaluation of mappers for MQAM and MAPSK USTLD systems

Following the discussion of the mapper optimisation criteria in Section 3.1, (9) indicates that higher metric scores (ζ) should be attained by mapper designs that achieve more labelling diversity. The aim of this substudy is to determine a quantifiable means of evaluating USTLD mappers, to get insight into the extent to which a mapper design achieves labelling diversity. Metrics that can be considered for this are given by (10)-(13), as derived in Section 3.1. To generalise

the result across different modulation schemes, a case study of MQAM USTLD systems is first presented. This is followed by evaluating the MAPSK USTLD mappers designed in this paper.

4.2.1 | Case study of BER performance of MQAM USTLD systems

The metric used by all previous MQAM USTLD mapper designs[16,22,23] is the minimum PED. The average BER performance of these mapper designs for 16QAM and 64QAM USTLD systems is shown in Figures 8 and 9, respectively. Similar studies

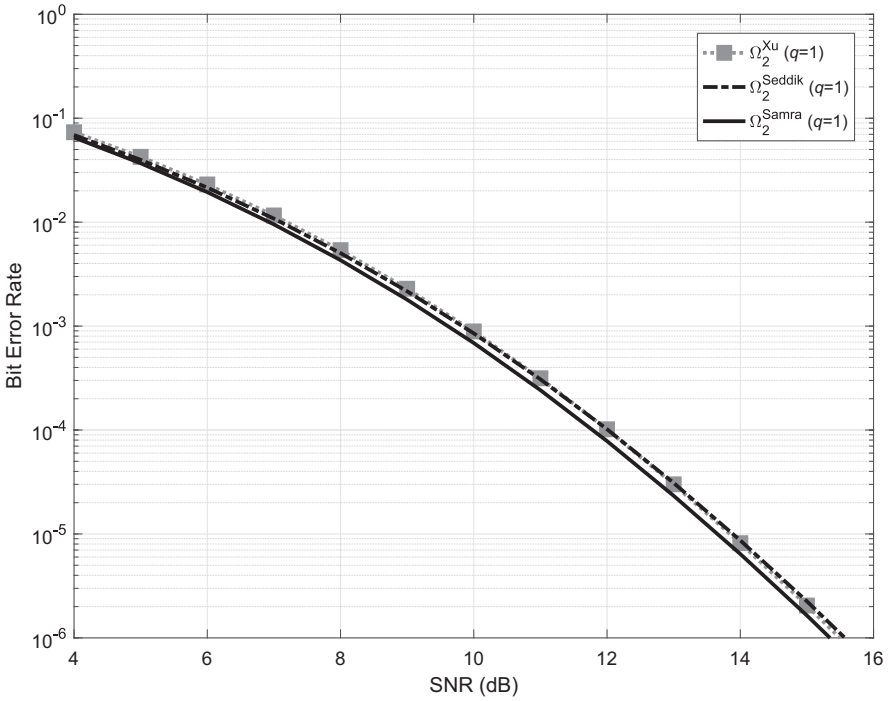

FIGURE 8 Average BER - 16QAM, Nakagami-*q*, analytical. BER, bit error rate; SNR, signal-to-noise ratio

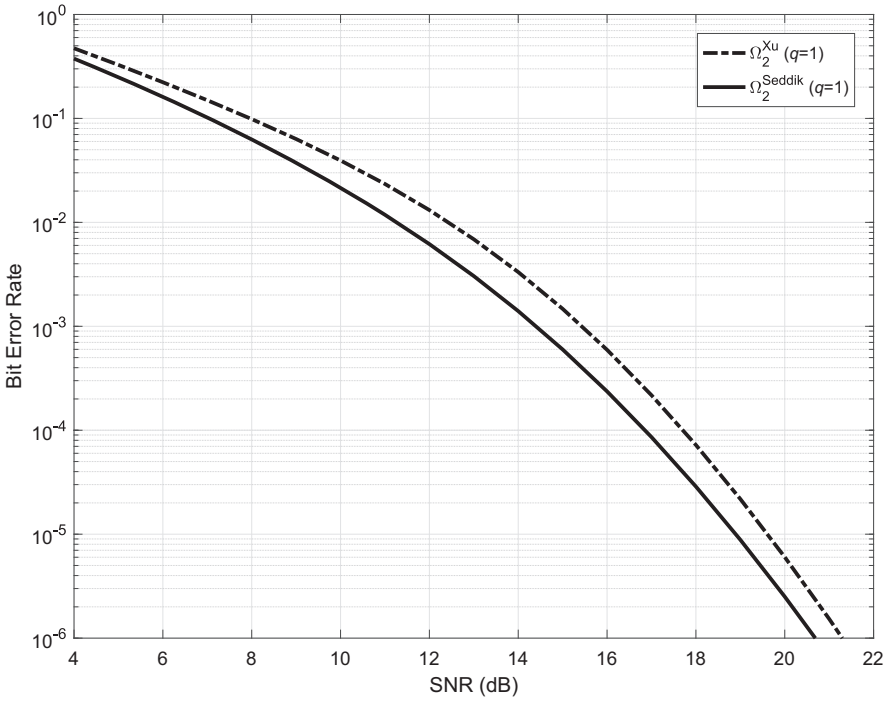

FIGURE 9 Average BER—64QAM, Nakagami-*q*, analytical. BER, bit error rate; SNR, signal-to-noise ratio

have been presented by Xu et al[16] and Quazi et al[28]; however, these works did not explain the reasons for the performance difference between the mapper designs.

From the BER curves in Figure 8, it can be seen that the mapper design Ω_2^{Samra} performs the best. This conclusion was also reached by similar BER comparison studies by Xu et al[16] and Quazi et al.[28] The performance of Ω_2^{Seddik} is shown to be the worst for 16QAM USTLD and best for 64QAM USTLD as shown in Figures 8 and 9, respectively. Figure 8 shows that the performance of Ω_2^{Xu} is shown to be worse than Ω_2^{Seddik} for SNR $\rho \leq$ 10dB, but better in the higher SNR region for 16QAM USTLD. However, overall, it is not better than Ω_2^{Samra}. Figure 9 shows that Ω_2^{Xu} performs worse than Ω_2^{Seddik} for 64QAM USTLD.

4.2.2 | Quantitative analysis of mappers

The optimisation problem statement in (9) indicates that larger values of a metric should correspond to better error performance. Given the discussions on the average BER performance in Sections 4.2.1 and 4.1 for MQAM and for MAPSK USTLD systems, respectively, the BER performance observations are summarised in Table 1. The related mathematical trends that are expected when comparing mappers are also presented.

The evaluation of the metrics $\zeta^{(1)}$ to $\zeta^{(4)}$ for MQAM USTLD is shown in Tables 2 and 3. Similarly, Tables 4 and 5 present the metric evaluations for the MAPSK USTLD systems considered.

From the metric scores for the minimum PED $\left(\zeta^{(1)}\right)$ in Tables 2 and 3, it can be seen that the scores achieved for all MQAM USTLD mapper designs are the same, ie, $\zeta^{(1)}_{\Omega_2^{\text{Samra}}} = \zeta^{(1)}_{\Omega_2^{\text{Seddik}}} = \zeta^{(1)}_{\Omega_2^{\text{Xu}}} = 8.0000$. However, the $\zeta^{(1)}$ scores for MAPSK follow the trends listed in points 3-5 above. Thus, the minimum PED is only appropriate in some cases and is inconclusive in others. In particular, it is unsuitable for comparing MQAM mappers. This indicates that the mappers designed by the heuristic approaches of Seddik et al[22] and Xu et al,[16] which were based on the minimum PED, can be further improved. This is especially true for higher-order modulation schemes as indicated by the results for 64QAM USTLD systems. As shown in Figure 9, Ω_2^{Seddik} shows $\approx$ 1 dB improvement over Ω_2^{Xu}, even though $\zeta^{(1)}_{\Omega_2^{\text{Seddik}}} = \zeta^{(1)}_{\Omega_2^{\text{Xu}}}$. This observation is expected as neither of these proposed mapper design techniques claimed that they produced a globally optimum secondary mapper.

The minimum bit-difference-weighted PED $\left(\zeta^{(2)}\right)$ shown in Tables 2 and 3 indicates that Ω_2^{Seddik} should perform the best for 16QAM and 64QAM. In Table 4, it is shown that $\zeta^{(2)}_{\Omega_2^{\text{Xu, QAM Based}}}$ has the lowest score and should perform worst for

TABLE 1 Summary of bit error rate (BER) performance observations and expected mathematical trends

Modulation	BER Performance Observations	Expected Mathematical Trends
16QAM	Ω_2^{Samra} performs the best and Ω_2^{Seddik} performs the worst	$\zeta_{\Omega_2^{\text{Seddik}}} < \zeta_{\Omega_2^{\text{Xu}}} < \zeta_{\Omega_2^{\text{Samra}}}$
64QAM	Ω_2^{Seddik} performs better than Ω_2^{Xu}	$\zeta_{\Omega_2^{\text{Xu}}} < \zeta_{\Omega_2^{\text{Seddik}}}$
16APSK	The performance of Ω_2^{Seddik} and Ω_2^{Samra} are approximately equal	$\zeta_{\Omega_2^{\text{Xu, PSK Based}}} < \zeta_{\Omega_2^{\text{Xu, QAM Based}}} < \zeta_{\Omega_2^{\text{Seddik}}}$,
	and are the best, and $\Omega_2^{\text{Xu, PSK Based}}$ performs the worst	$\zeta_{\Omega_2^{\text{Samra}}} \approx \zeta_{\Omega_2^{\text{Seddik}}}$
64APSK	Ω_2^{Seddik} performs the best and $\Omega_2^{\text{Xu, QAM Based}}$ performs the worst	$\zeta_{\Omega_2^{\text{Xu, QAM Based}}} < \zeta_{\Omega_2^{\text{Xu, PSK Based}}} < \zeta_{\Omega_2^{\text{Seddik}}}$

TABLE 2 Metric values for 16QAM

Mapper	$\zeta^{(1)}$	$\zeta^{(2)}$	$\zeta^{(3)}$	$\zeta^{(4)}$
Ω_2^{Samra}	8.0000	2.9814	248.5534	126.2967
Ω_2^{Seddik}	8.0000	4.0000	249.3607	124.5856
Ω_2^{Xu}	8.0000	2.9814	167.5542	87.7028

TABLE 3 Metric values for 64QAM

Mapper	$\zeta^{(1)}$	$\zeta^{(2)}$	$\zeta^{(3)}$	$\zeta^{(4)}$
Ω_2^{Seddik}	8.0000	4.0000	3102	1050
Ω_2^{Xu}	8.0000	2.8844	2651	928.0312

TABLE 4 Metric values for 16APSK

Mapper	$\zeta^{(1)}$	$\zeta^{(2)}$	$\zeta^{(3)}$	$\zeta^{(4)}$
Ω_2^{Samra}	5.5991	2.0179	155.1395	78.3989
Ω_2^{Seddik}	5.5991	2.0000	155.5276	78.2538
$\Omega_2^{\text{Xu,QAM Based}}$	4.0000	1.4907	116.0646	62.7097
$\Omega_2^{\text{Xu,PSK Based}}$	2.0000	2.0000	120.3336	60.5295

TABLE 5 Metric values for 64APSK

Mapper	$\zeta^{(1)}$	$\zeta^{(2)}$	$\zeta^{(3)}$	$\zeta^{(4)}$
Ω_2^{Seddik}	5.0262	1.6100	1757	580.1394
$\Omega_2^{\text{Xu,QAM Based}}$	1.5434	0.9800	1796	651.2771
$\Omega_2^{\text{Xu,PSK Based}}$	1.5434	0.9800	1844	637.9502

16APSK. However, this is contrary to the results in Figure 8 for 16QAM and Figure 6 for 16APSK. Thus, this metric is misleading and should not be used for comparing USTLD mappers.

The summed PED metrics $\left(\zeta^{(3)}\text{and}\zeta^{(4)}\right)$ for 16QAM are inconclusive as $\zeta^{(i)}_{\Omega_2^{\text{Seddik}}} \approx \zeta^{(i)}_{\Omega_2^{\text{Samra}}}, i \in [3:4]$. However, for 64QAM, both these metrics correctly rank Ω_2^{Seddik} higher than Ω_2^{Xu}. Thus, either $\zeta^{(3)}\text{or}\zeta^{(4)}$ can be used to compare higher-order modulation USTLD mappers using MQAM. In the context of MAPSK, $\zeta^{(4)}$ gives the correct result in 16APSK, but not in 64APSK. $\zeta^{(3)}$ ranks the mapper designs incorrectly for both 16APSK and 64APSK. However, in cases where $\zeta^{(1)}$ is equal, $\zeta^{(3)}$ gives the correct ranking for the considered subset of mappers being compared. This observation thus motivates for a two-stage approach for comparing mapper designs. In the first stage, the minimum PED $\left(\zeta^{(1)}\right)$ of the considered mapper designs should be compared. If these are found to be equal, then in the second stage, $\zeta^{(3)}$ can be used to rank them. For each of the 16-ary and 64-ary QAM and APSK USTLD systems studied in this paper, the two-stage approach results in the correct ranking of the mappers designs.

5 | CONCLUSION

This paper presents a USTLD system design for mobile satellite communication systems using MAPSK constellations from the latest DVB-S2X standard. A novel approach to MAPSK USTLD mapper design is presented, based on existing MQAM designs. The proposed mapper designs rely on the observation that MQAM and MAPSK constellations consist of symbols arranged in a series of concentric squares and circles, respectively. This constrains the MAPSK constellations to only the 4+12 16APSK and 4+12+20+28 64APSK configurations. The results from a study of the average BER of the MAPSK USTLD system show gains of approximately 4 dB and 5 dB for 16APSK and 64APSK, respectively, when compared to a similar existing STBC system. The study was conducted using both theoretical and simulation results assuming Nakagami-q fading channels.

A second study is conducted to develop an analytical approach to comparing USTLD mapper designs. The objective of this study is to determine a suitable metric for use in the design optimisation criteria. Four metrics based on the minimum PED are derived from the analytical expression for the average BER performance of the system. The result of the average BER performance is used to investigate the suitability of these metrics. The study considers MQAM and MAPSK to propose a more generic mapper design comparison methodology. The results show that none of the metrics are individually suitable, motivating for a two-stage approach. In the first stage, the minimum PED of the considered mapper designs are compared. In cases where these are found to be equal, a second stage is introduced wherein the minimum summed PED is used to rank them. This approach is shown to correctly rank the MQAM and MAPSK USTLD mapper designs considered in this paper.

In future work, a generic mapper design algorithm can be developed for USTLD systems. This can be used to consider the complete set of DVB-S2X MAPSK constellations, as this paper only considers the 4+12 16APSK and 4+12+20+28 64APSK configurations. The USTLD mapper design comparison methodology presented in this paper can be used to develop a framework within which such an algorithm can be designed.

ORCID

Tahmid Quazi https://orcid.org/0000-0002-1288-4224
Sulaiman Saleem Patel https://orcid.org/0000-0003-3557-3645

REFERENCES

1. Nwulu NI, Adekanbi A, Oranugo T, Adewale Y. Television broadcasting in Africa: Pioneering milestones. Paper presented at: Second Region 8 IEEE Conference on the History of Communications; 2010; Madrid, Spain. https://doi.org/10.1109/HISTELCON.2010.5735315
2. Yesufu AK. Possible use of satellites in rural telecommunications in Africa. Paper presented at: Second International Conference on Rural Telecommunications; 1990; London, UK.
3. Mbarika VW, Byrd TA. An exploratory study of strategies to improve Africa's least developed economies' telecommunications infrastructure: the stakeholders speak. *IEEE Trans Eng Manag*. 2009;56(2):312-328.
4. Tomassini D, Ginati A, Feliciani F, et al. Space4edu: Satellite technology for smart rural schools in South Africa. Paper presented at: 64th International Astronautical Congress; 2013; Beijing, China.
5. Martín-de-Mercado G, Horsch A, Parentela G, Mancini P, Ginati A. Satellite-enhanced telemedicine and eHealth for sub-Saharan Africa: A development opportunity. Paper presented at: 62nd International Astronautical Congress; 2011; Cape Town, South Africa.
6. Olla P. Exploiting satellite radio technology to create an African satellite health education infrastructure. Paper presented at: 57th International Astronautical Congress; 2006; Valencia, Spain.
7. Iqbal MK, Iqbal MB, Shamoon S, Bhatti M. Future of satellite broadband Internet services and comparison with terrestrial access methods e.g. DSL and cable modem. Paper presented at: 3rd IEEE International Conference on Computer, Control and Communication; 2013; Karachi, Pakistan. https://doi.org/10.1109/IC4.2013.6653763
8. Conte R. Satellite rural communications: telephony and narrowband networks. *Int J Satell Commun Netw*. 2005;23(5):307-321.
9. Aiyetoro G, Takawira F, Walingo T. Near-optimal packet scheduling scheme in satellite LTE networks. *IET Communications*. 2017;11(15):2311-2319.
10. Ravishankar C, Noerpel A, Jong JJ, et al. Design and performance of an all-Internet Protocol mobile satellite system. *Int J Satell Commun Netw*. 2015;33(4):329-349.
11. Peters G. Satellite delivery of next generation broadband access to the UK. Paper presented at: 5th Advanced Satellite Multimedia Systems Conference and the 11th Signal Processing for Space Communications Workshop; 2010; Cagliari, Italy. https://doi.org/10.1109/ASMS-SPSC.2010.5586871
12. Markhasin A. Ubiquitous and multifunctional mobile satellite all-IP over DVB-S networking technology 4G with radically distributed architecture for RRD regions. Paper presented at: International Workshop on Satellite and Space Communication; 2007; Salzburg, Austria. https://doi.org/10.1109/IWSSC.2007.4409398
13. Arapoglou P-D, Liolis K, Bertinelli M, Panagopoulos A, Cottis P, De Gaudenzi R. MIMO over satellite: a review. *IEEE Commun Surv Tutor*. 2011;13(1):27-51.
14. Arti MK, Jindal SK. OSTBC transmission in shadowed-Rician land mobile satellite links. *IEEE Trans Veh Technol*. 2016;65(7):5771-5777.
15. Alamouti SM. A simple transmit diversity technique for wireless communications. *IEEE J Sel Areas Commun*. 1998;16(8):1451-1458.
16. Xu H, Govindasamy K, Pillay N. Uncoded space-time labelling diversity. *IEEE Commun Lett*. 2016;20(8):1511-1514.
17. Huang Y, Ritcey JA. Improved 16-QAM constellation labelling for BI-STCM-ID with the Alamouti scheme. *IEEE Commun Lett*. 2005;9(2):157-159.
18. Krasicki M. Improved labelling diversity for iteratively-decoded multi-antenna systems. Paper presented at: 7th International Conference on Wireless Communications and Mobile Computing IWCMC; 2011; Istanbul, Turkey.
19. Krasicki M. Essence of 16-QAM labelling diversity. *IET Electron Lett*. 2013;49(8):567-569.
20. Dlodlo B, Xu H. Trellis code-aided high-rate M-QAM space-time labeling diversity using a unitary expansion. *Int J Commun Syst*. 2018;31(11):e3590. https://doi.org/10.1002/dac.3590
21. Ejaz S, Yang F, Xu H. Labeling diversity for 2 × 2 WLAN coded-cooperative networks. *Radioengineering*. 2015;24(2):470-480.
22. Seddik KG, Ibrahim AS, Liu KJR. Trans-modulation in wireless relay networks. *IEEE Commun Lett*. 2008;12(3):170-172.
23. Samra H, Ding Z, Hahn P. Symbol mapping diversity design for multiple packet transmissions. *IEEE Trans Commun*. 2005;53(5):810-817.
24. Govindasamy K, Xu H, Pillay N. Space-time block coded spatial modulation with labelling diversity. *Int J Commun Syst*. 2017:e3395. https://doi.org/10.1002/dac.3395
25. Pillay N, Xu H. Uncoded space-time labelling diversity – application of media-based modulation with RF mirrors. *IEEE Commun Lett*. 2018;22(2):272-275.
26. Patel SS, Quazi T, Xu H. High-rate uncoded space-time labelling diversity with low-complexity detection. *Trans Emerging Tel Tech*. 2018. Under review.
27. Patel SS, Quazi T, Xu H. Error performance of uncoded space time labelling diversity in spatially correlated Nakagami-q channels. *Int J Commun Syst*. 2018;31(12):e3720. https://doi.org/10.1002/dac.3720
28. Quazi T, Xu H. SSD-enhanced uncoded space-time labelling diversity. *Int J Commun Syst*. 2018;31(11):e3592. https://doi.org/10.1002/dac.3592

29. Quazi T, Xu H. BER performance of a hierarchical APSK UEP system over Nakagami-m fading channels. *SAIEE Afr Res J*. 2016;107(4):230-236.
30. Park B, Jin S, Jeong D, et al. Highly linear mm-Wave CMOS power amplifier. *IEEE Trans Microw Theory Tech*. 2016;64(12):4535-4544.
31. Digital Video Broadcasting. Second generation framing structure, channel coding and modulation systems for Broadcasting, Interactive Services, News Gathering and other broadband satellite applications; Part 2: DVB-S2 Extensions (DVB-S2X). European Telecommunications Standards Institute. EN 302 307-2 V1.1.1; 2014.
32. Morello A, Mignone V. DVB-S2: the second generation standard for satellite broad-band services. *Proc IEEE*. 2006;94(1):210-227.
33. Chytil B. The distribution of amplitude scintillation and the conversion of scintillation indices. *J Atmospheric Terr Phys*. 1967;29(9):1175-1177.
34. Simon MK, Alouini M-S. *Digital Communication over Fading Channels: A Unified Approach to Performance Analysis*. New York, NY: John Wiley & Sons Inc; 2000.
35. Sung W, Kang S, Kim P, Chang D, Shin D-J. Performance analysis of APSK modulation for DVB-S2 transmission over nonlinear channels. *Int J Satell Commun Netw*. 2009;27(6):295-311.
36. Meloni A, Murroni M. On the genetic optimization of APSK constellations for satellite broadcasting. Paper presented at: 2014 IEEE International Symposium on Broadband Multimedia Systems and Broadcasting; 2014; Beijing, China.
37. Anedda M, Meloni A, Murroni M. 64-APSK constellation and mapping optimization for satellite broadcasting using genetic algorithms. *IEEE Trans Broadcast*. 2016;62(1):1-9.
38. Chen X, Yang H. Optimization of MAPSK. Paper presented at: 11th International Conference on Advanced Communications Technologies ICACT; 2009; Phoenix Park, South Korea.

How to cite this article: Quazi T, Patel SS. USTLD mapper design for APSK constellations over satellite links. *Trans Emerging Tel Tech*. 2019;e3586. https://doi.org/10.1002/ett.3586